JOM 23501

A model for CO insertion in transition metal complexes

A.L. Tchougreeff, Yu.V. Gulevich and I.A. Misurkin

Karpov Institute of Physical Chemistry, 103064, Moscow (Russian Federation)

I.P. Beletskaya

Department of Chemistry, Moscow State University, Moscow (Russian Federation)

(Received December 9, 1992)

Abstract

A theoretical model recently developed for describing reactions catalysed by transition metal complexes is applied to CO insertion in RML_n complexes (where M is a transition metal, R is aryl, alkyl, or another σ-bonded ligand, and L stands for ancillary ligands). The effect of the migrating group R, the metal M, and the number of ancillary ligands L on the insertion step is studied. The mechanism of the double carbonylation reactions of organic halides, catalysed by transition metal complexes, is analysed in the framework of the proposed model.

1. Introduction

Carbonyl monoxide insertion into the transition metal–carbon σ-bond is the central step of a number of catalytic carbonylation reactions used for the syntheses of both industrial and fine chemicals [1–4]. For these reasons, insertion of the CO molecule has become the subject of numerous experimental [1–7] and theoretical [8–20] studies.

Two aspects of this reaction are of particular interest to theoreticians. First, they are interested in the particular type of nuclear motion (reaction path) which leads from the original alkyl or aryl metal derivatives to acyl complexes. It has been shown [8] with use of the extended Hückel theory (EHT) that for prototypic CO insertion, leading to acetyl in the coordination sphere of methylpentacarbonylmanganese [5], the actual nuclear motion is the migration of the σ-coordinated axial CH_3 group towards one of the equatorial CO ligands. A similar migration has been found to be the reaction coordinate for CO insertion in the complexes $RM(CO)L_2X$ where M = Pd and Pt [13,15].

The second problem of interest to theoreticians, and which is of particular interest to us, was to find out the qualitative features of the electronic structure of σ-bonded groups and those of fragments containing transition metal that determine the activation energy of the CO insertion step.

It might seem to be very natural to correlate the energy of the M–R bond and the rate of the CO insertion into that bond, (the weaker the bond, the easier the migration proceeds), and attempts to rationalize the CO insertion step in terms of bond strength are numerous (for review see [7]). However, experimental facts contradict this simple picture. For example, the energy of the $Mn–COCH_3$ bond is even slightly less than that of the $Mn–CH_3$ bond, but acyl ligands are unable to migrate to the coordinated CO. The same is true for CF_3 and Ph ligands. Their bond energies are almost equal but carbonylation occurs for the Ph ligand only [7].

Another approach, rationalizing the insertion in terms of basicity–acidity, turned out to be more promising. Direct EHT calculations [8] showed that the increase in the energy of the σ-lone pair orbital of R^- (*i.e.* the increase in its basicity and correspondingly the decrease in the ionization potential) favours the reaction. That result has been confirmed subsequently [15,19] at the *ab initio* level.

The purpose of this paper is to analyse the features of electronic structure affecting the CO insertion into

Correspondence to: Dr. I.P. Beletskaya.

0022-328X/93/$6.00

the metal–carbon bond in terms of a general configuration interaction (CI) method [21,22], which was especially designed to analyse transformations of molecules in ligand spheres of transition metal complexes. We clarify the reasons for the validity of the basicity–acidity criteria and indicate their limitations. We also propose a numerical index for the migrative capacity of σ-bonded groups and apply it to distinguish that capacity for the groups with close M–R energies.

2. Synopsis of the method

The method [21,22] starts from a very general assumption (see also refs 23,24) that the ground state wave function Ψ_G of a complex containing reacting ligands can be presented as a superposition of two electronic configurations (resonance structures):

$$\Psi_G = a\Psi_u + b\Psi_r \qquad (1)$$

$$(a^2 + b^2 = 1)$$

and thus the energy profile (EP) for the reaction also becomes a superposition of the EPs for the two resonance structures. The above representation of the ground state wave function is absolutely trivial, unless the selection procedure for the configurations Ψ_u and Ψ_r is not especially designed [21,22] to analyse the behaviour of coordinated molecules. This procedure comprises three steps.

The first step is to learn if the barrier exists in the EP of the reaction between free (non-coordinated) reagents in their ground state. If so the ground state can be considered as an unreactive state. The electronic configuration Ψ_u in the above expansion for the ground state of the entire complex is then taken as the product of the ground state of the metal with ancillary ligands and the unreactive ground state of the reagents. It has been shown [21,22,25] that under certain conditions, the shape of the EP for the configuration Ψ_u is similar to that for the ground state of free reagents and also increases along the reaction path.

The second step is to find the excited and/or ionized states of free reagents, which have a relatively low barrier in the EP for the reaction considered. These states (if any exist) are referred to as reactive states. The configuration Ψ_r in that case is taken as the product of some excited and/or ionized state of the metal with ancillary ligands and one of the reactive state of the reagents. The shape of the EP for the Ψ_r configuration coincides with that for the reactive excited or/and ionized states of free reagents [21,22,25] and thus increases slowly along the reaction path.

The third step is to consider the fragment of the entire catalytic complex that comprises the transition metal atom and ancillary ligands (the fragment is obtained by removing the reagents from the whole complex) and answer the question whether it is able to coordinate free reagent molecules; if so will some reactive configurations (Ψ_r) be admixed to the unreactive configuration (Ψ_u), *i.e.* will the expansion coefficient b in eqn. (1) be non-zero. If some reactive configuration is admixed, the above two configurational expansions, eqn. (1), becomes non-trivial and the EP for the transformation of the complex corresponding to the reaction of coordinated reagents depends upon the weight of the configurations (b^2 and a^2). The greater the weight of the reactive configuration (b^2), the lower the barrier for the reaction.

2.1. Origin of the barrier in CO insertion

Now we apply the general method briefly outlined above to the CO insertion step. We must first consider the reaction between free CO and R^-. However, such an analysis has already been performed by Berke and Hoffmann [8]. They have found that the dominating contribution to the total energy, which increases along the reaction path, is the four-electron destabilizing interaction between the lone pair orbitals σ_R and σ_{CO}; it is responsible for the barrier formation (see also [26]). The same type of interaction is responsible for repulsion of two helium atoms; the exchange repulsion of two occupied orbitals. The EP for the approach of R^- and CO is shown in Scheme 1. Clearly, the state $\sigma_{CO}^2\sigma_R^2$ is the unreactive state of the reagents. Thus, the first step of our program has already been performed in [8].

The next step of the selection procedure [21,22] is to find the reactive state where the approach of R and CO is barrierless. The simplest idea proposed in [25] is to remove an electron from the σ_R orbital and to consider the reaction of the $R^{\cdot}$ radical with CO. This strategy for searching for the reactive state can be based on the above analogy with two helium atoms (see also [27]). Although the ground state EP for two neutral atoms of helium (a system with four electrons) has no minima, and they repel each other, the EP for He and He^+ (a system with three electrons) is attractive

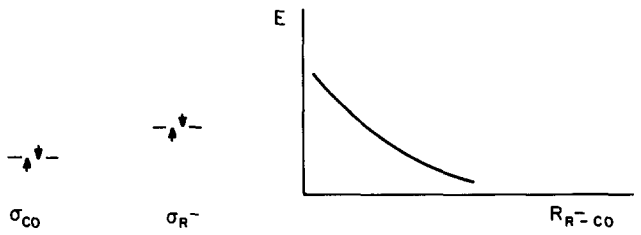

Scheme 1.

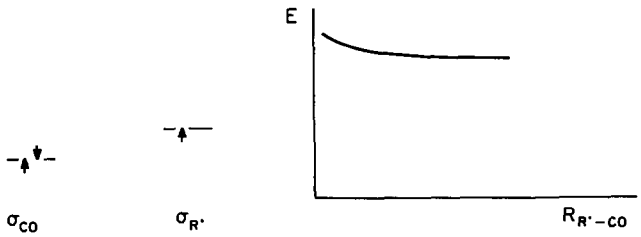

Scheme 2.

(the molecular ion He_2^+ is stable).] The EP for the reaction of R˙ and CO is not attractive, but according to calculations performed in [25], it is only weakly repulsive. The state $\sigma_{CO}^2\sigma_R^1$ is clearly the state with low barrier, *i.e.* the reactive state, which we had to find at the second step of our configuration selection procedure.

In order to perform the third step of our analysis, we consider the effect of a ML_n^+ fragment on the reaction between R^- and CO. In our case, the barrier in the ground state arises due to four-electron repulsion. The unique way to remove it and to transform this state into the reactive one is obviously to transfer an electron from the reagents to the ML_n^+ fragment [25]. The same idea was recently applied to the problem of the surface assisted Xe–Xe bonding in [27], where the whole metal surface was assumed to be part of the ML_n^+ fragment.

Now we are in a position to construct the configurations Ψ_u and Ψ_r. We consider explicitly only one empty orbital (M) of ML_n^+. All the occupied orbitals of the ML_n^+ fragment are treated as a frozen core. To describe electrons on the reagents, we consider explicitly the two lone pair orbitals σ_{CO} and σ_R. Other occupied orbitals of both R^- and CO are also treated as a frozen core, and other empty orbitals are disregarded. Then the two configurations participating in the expansion eqn. (1) are $\Psi_u = [\text{core}]\sigma_{CO}^2\sigma_R^2$ corresponding to the $[R^- + CO][ML_n^+]$ state (resonance structure) of the $RM(CO)L_n$ complex and $\Psi_r = [\text{core}]\sigma_{CO}^2\sigma_R^1M^1$ with one electron transferred to the fragment orbital M, corresponding to the $[R^{\cdot} + CO][ML_n]$ state. The EP for the $[R^- + CO][ML_n^+]$ state resembles that of the reaction of free R^- and CO and thus the configuration Ψ_u is the unreactive one. Similarly the EP for the $[R^{\cdot} + CO][ML_n]$ state, the shape close to that of the reaction of free R˙ with CO and the configuration Ψ_r, is reactive.

The configurations Ψ_u and Ψ_r are mixed due to resonance interaction between the reagents (R + CO) and the ML_n fragment. The degree of mixing of the two configurations depends on the difference in their energies Δ and on the resonance parameter β which reflects the intensity of one-electron transfer between the reagents (R + CO) and the ML_n^+ fragment. The parameter Δ is estimated by

$$\Delta = IP - EA + C$$

where IP is the energy of abstraction of an electron from the R^- lone pair orbital, EA is the electron affinity of ML_n^+ and C is the energy of the Coulomb attraction between an electron in the R^- lone pair and the ML_n^+ fragment. According to the general rules of quantum mechanics, the degree of mixing (when it is not very large) is given by the relation

$$b/a = (\beta/2\Delta)$$

The mixing of Ψ_u and Ψ_r gives the ground state of the complex Ψ_G. The ground state energy of the complex is lower than the energies of both the $[R^- + CO][ML_n^+]$ (Ψ_u) and $[R^{\cdot} + CO][ML_n]$ (Ψ_r) states (Scheme 3). When b/a is not very large, the energy of the ground state Ψ_G is lower than that of the Ψ_u state by the term $-\beta^2/|\Delta|$. This stabilization occurs at any point along the reaction path and the smaller the energy difference Δ between the Ψ_u and Ψ_r states, the larger is the stabilization. The slope of the resulting EP is intermediate (Scheme 3); it is smaller than that for the unreactive state and larger than that for the reactive state. Thus the EP of the CO insertion into the M–R bond below that for the reaction of free R^- and CO and has a smaller slope. Because of the smaller slope, the barrier is also lowered for CO insertions in the coordination sphere of the transition metal complex, compared with the hypothetical reaction between free R^- and CO.

To summarize the above analysis (see also [25]) of the CO insertion reaction in the ligand sphere of transition metal complexes, we can state that the activation energy of the insertion step originates from the exchange repulsion between the lone pairs of R^- and CO. The barrier of the intraspheric reaction depends on the contributions a^2 and b^2 of the $[R^- + CO][ML_n^+]$ (Ψ_u) and $[R^{\cdot} + CO][ML_n]$ (Ψ_r) configurations to the ground state Ψ_G of the entire complex. The larger the contribution of the Ψ_u state, the higher the barrier.

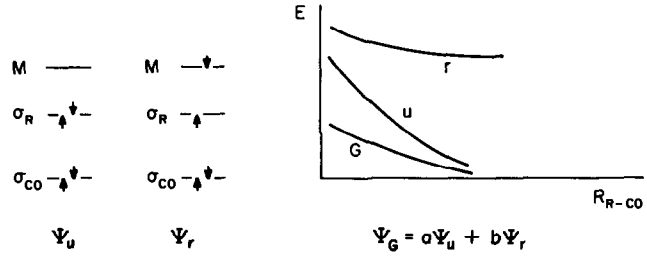

Scheme 3.

Conversely, the larger the contribution of the Ψ_r state, the lower the barrier. In order to analyze the effect of different factors upon the EP of the insertion, we propose several numerical indices. In the subsequent sections, we discuss these indices, check their validity and apply them to an analysis of some experimental situations.

3. Effective ionization potentials and migrative capacity of R^-

As can be seen from the analysis performed in the previous section, the IP controls the slope of the EP of the insertion reaction through variations of the contribution from the reactive and unreactive configurations to the ground state. A decrease in IP increases the contribution of the reactive configuration and thus lowers the barrier of the reaction. The question is what particular quantity is to be taken as the IP for the analysis of reactivity. An obvious possibility is to take the experimental ionization potential I_{exp} of the R^- anion. However, in this case we encounter the well-known contradiction (see [28] for a detailed discussion) between the local character of the chemical interaction and delocalization of the molecular orbitals. The experimental IP (I_{exp}) corresponds to abstraction of an electron from an MO delocalized over the whole molecule. The chemical interaction, in contrast, has local character; thus it seems more appropriate to take as an index for the reactivity of the lone pair, involved in the interaction, some quantity that reflects the local character of the lone pair.

An alternative method is to find the hybride orbitals σ_R and σ_{CO} of the lone electronic pairs (HOLE) for R^- and CO as an expansion over the MOs of the corresponding molecules in some approximation and consider their ionization potentials. The effective IP I_{eff} for the HOLE has the form [25,29]

$$I_{eff} = -\sum_i \left(C_i^{HOLE}\right)^2 \epsilon_i$$

where C_i^{HOLE} is the coefficient of the ith MO in the expansion of the hybrid orbital of the lone pair and ϵ_i is the orbital energy of the ith MO.

In Table 1, the experimental IP (I_{exp}) [30] and the effective IP (I_{eff}) for the aryl anions $Ar^- = Y\text{-}C_6H_4^-$ are presented together with data on their migrative capacity [31]. The effective IP I_{eff} is a measure of the donor capacity of the lone pair (for more details see [29]). Note, however, that anions with large I_{exp} also have large I_{eff} and *vice versa*.

Both the characteristics (I_{exp} and I_{eff}) of aryl anions correlate with the experimental rate of transformation of $ArM(CO)L_2X$ to $ArCOML_2X$ [31] (here M is Ni, Pd, or Pt; X stands for halogen, and L are organophosphine or -arsine ligands). In general, the ability of aryl ligands to migrate to coordinated CO increases with decrease in IP of the corresponding anion Ar^-. Based on the values of IPs, we expect the rate of the insertion into the M–Alk bond to be larger than that of the insertion into the M–Ar bond. As a rule, aromatic ligands Ar^- with electron-donating substituents migrate more easily than those with electron-withdrawing substituents.

The effective IP (I_{eff}) clearly distinguishes the reactivity (migrative capacity) of different groups with close M–R bond energies. As has been pointed out in the Introduction, the bond energies of the Ph and CF_3 ligands are close, but their capacities to migrate to coordinated CO differ drastically. Their I_{eff}, however, differ strongly (see Tables 1, 2) and according to our picture, this explains the observed difference in reactiv-

TABLE 1. Ionization potentials (eV) of substituted aryl anions $Y\text{-}C_6H_4^-$ together with some data on their migrative capacity

Y	I_{exp} [a]	I_{eff} [b]	$10^4\,k_{obsd}$ [c] (s^{-1})	$10^4\,k_2$ [d] (s^{-1})
H	2.2	7.5	35 [f]	7.4
O_2N	2.42	8.6	1.15 [e]	–
			1.86 [g]	
NC	–	7.9	2.10 [e]	–
			4.10 [g]	
F_3C	–	8.6	9.6 [g]	–
Cl	2.43	8.1	–	6.5
H_3C	–	7.6	> 100 [f]	8.3
H_3CO	–	–		12.1

[a] Experimental IPs from [30]. [b] Effective IPs for lone pair orbitals calculated in [25]. [c] Measured in [31] by the rate of CO absorption under 1 atm of CO. [d] Measured in [31] for insertion in the $YC_6H_4Pt((4\text{-}CH_3C_6H_4)_3P)_2I$ complex under excess phosphine at 43.6°C. [e] Measured in [31] for insertion in the $YC_6H_4Pd((C_6H_5)_3P)_2Cl$ complex at 43.2°C. [f] Measured in [31] for insertion in the $YC_6H_4Pd((C_6H_5)_3P)_2Br$ complex at 2.3°C. [g] Measured in [31] for insertion in the $YC_6H_4Pd((C_6H_5)_3P)_2Br$ complex at 43.2°C.

TABLE 2. Ionization potentials (eV) of some R^- anions

R	I_{exp} [a]	I_{eff} [b]	R	I_{exp}	I_{eff}
C_6H_5CO	–	10.7	CF_3	2.7	12.1
$O_2NC_6H_4CO$	–	11.0	CF_2H	–	10.8
			$Me_2C{=}C(OH)$	–	8.7
NCC_6H_4CO	–	10.5			
			Me_2CHCO	–	11.1
CH_3	1.1	3.5			
			J	3.08	–
CH_3CH_2	0.9	–	Cl	3.61	–
MeO	0.38 ÷ 1.5	6.7	Me_2N	1.04	6.9
C_6H_5O	1.2	8.3			
HO	1.83	–			

[a] Experimental IPs from [30]. [b] Effective IPs for lone pair orbitals calculated in [25].

ity. The IP for CF_3^- is very large and therefore its migration must be restricted in accordance with experiment.

The effective IP calculation [25] also showed that I_{eff} of the acyl anions is considerably higher than that of the alkyl and even of the less reactive aryl anions (see Tables 1, 2). Thus, according to our approach, CO insertion into the M–COR bond is unfavourable, in fair agreement with experiment.

Up to this point, we have considered only the migratory CO insertion into the metal–carbon bond. However, the principles formulated above are useful for estimating the ability of any σ-bonded ligands to migrate to coordinated CO. Among them, RO^- and R_2N^- are the most important [32]. Their IPs and hence their capacity to migrate to CO are close to those of alkyls and aryls (see Table 2). For that reason, the CO insertion into the M–O or M–N bond might take place if the corresponding intermediates containing CO together with amide or alcoholate anion ligand were detected.

Another important example of the migration of a non-carbanion ligand to coordinated CO is that provided by the hydride anion. It is considered to be a central step of a number of carbonylation processes [1–3]. However, only a few examples of formyl complex formation which can be unequivocally attributed to the CO insertion into the metal–hydrogen bond, are known [3,33]. Therefore, the situation is not clear from the experimental point of view. However, our model allows us to make some statements. The experimental IP of the H^- anion amounts to 0.75 eV [30]. According to our model, this value indicates that the CO insertion into the M–H bond should proceed easily. On the other hand, the quantum chemical calculations [12,16,17] unanimously testify that the barrier for hydride migration is significant. For an analysis of this obvious discrepancy between our qualitative model and the calculations [12,16,17], see below.

The IPs of the halogen anions are high: the values of I_{exp} for Cl^- and J^- are 3.61 eV and 3.08 eV, respectively (the effective IP cannot be calculated in these cases [29]). Thus, CO insertion into the M–Hal bond is restricted. This is in agreement with the observation that carbonylation of $ArML_2Hal$ complexes yields only $ArCOML_2Hal$ which are products of insertion into the Ar–M bond [6,31]. Any products of CO insertion into the M–Hal bond have never been found. Thus, the ligands with I_{exp} smaller than or about 2.3 eV migrate to CO.

To summarize, generally the IPs of the R^- ligands correlate fairly well with their ability to migrate to coordinated CO. We conclude that migration occurs if the donor capacity index I_{eff} of R^- is lower than 9–10 eV. For the experimental IPs (I_{exp}), this threshold lies somewhere between 2.5 and 3 eV.

3.1. Double carbonylation

The carbonylation of aryl or alkyl complexes RML_n yields acyl complexes $RCOML_n$. One might expect that the insertion of the second CO molecule into the metal–acyl (M–COR) bond of $RCOML_n$ would give the acylformyl complexes $RCOCOML_n$. However, all attempts to prepare $RCOCOML_n$ by the reaction of $RCOML_n$ with CO have been unsuccessful (see for example [34]). From our point of view, it is the relatively high values for the effective IPs for acyl anions (see above) which explains this result.

The situation seems to change if the tautomeric transformation of the acyl ligand into its enolic form is possible. It has been shown [35] that the enolization of the intermediate acyl complex $PhCHRCOCo(CO)_4$ takes place in the course of double carbonylation of benzyl halides promoted by $Co_2(CO)_8$. The enolization is followed by insertion of the second CO molecule leading to formation of the enolic form of the acylformyl complex $PhCR{=}C(OH)COCo(CO)_4$ (Scheme 4).

This mechanism can be supported in the framework of our approach to the CO insertion reaction. The acyl ligands do not migrate to coordinated CO because of large effective IPs of the corresponding anions RCO^-. The values of I_{eff} for the enolic forms of the same anions are considerably lower. For example, the I_{eff} values calculated for the acylic (Me_2CHCO^-) and enolic ($Me_2C{=}C(OH)^-$) forms of the model anion are 11.1 eV and 8.7 eV, respectively (see Table 2). Hence the enolized acyl ligand is able to migrate to coordinated CO in perfect agreement with experiment.

As the second example, we consider the synthesis of α-ketoacids and their derivatives ArCOCONu (Nu =

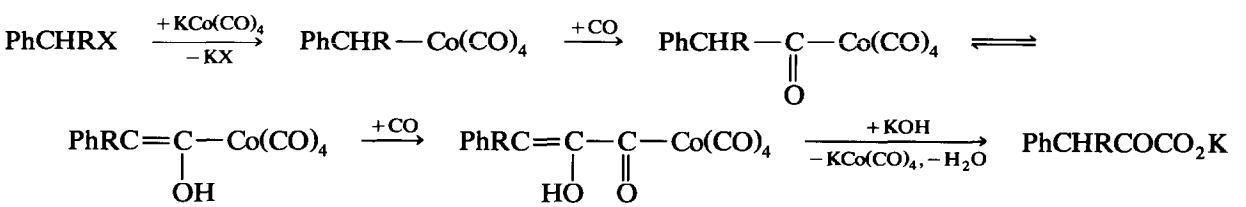

Scheme 4.

OR, NR_2) by carbonylation of aryl halides ArX in the presence of nucleophiles HNu, catalysed by palladium complexes. Two alternative mechanisms can be proposed for this reaction [4] (Scheme 5).

As we know, CO insertion into the Pd–COAr bond is restricted and therefore path B is unfavoured. The present theoretical model supports path A. Path A has also been confirmed experimentally [4,33,34]. It is worthwhile to note that the insertion into the Pd–Nu bond might proceed with ease due to low (of about 6.5–7.0 eV) values of I_{eff} for the Nu^- anions if intermediate complexes of the type $ArCOPd(CO)NuL_2$ occur in the course of the reaction [25].

4. Effect of the ML_n^+ fragment on CO insertion

Now we consider the effect of the metal and also of the number and the type of ancillary ligands L on CO insertion in $RM(CO)L_n$ complexes. We have pointed out before that the height of the barrier on the reaction path depends on the relative contribution from the reactive and unreactive configurations to the ground state of the complex. Clearly, the electron affinity (EA) of the ML_n^+ fragment can affect them. The greater EA is, the lower must be the activation energy. However, it is not an easy problem in general to estimate EA and moreover, it is not the unique factor controlling the weights of the reactive and unreactive configurations. Another factor is the magnitude of the resonance parameter β, reflecting the intensity of one-electron transfers between reagents and the metal-containing fragment (see above). Hence, in order to estimate the contributions to the ground state, we performed fragment MO analysis [36] in the framework of the general EHT method [37] (FMO-EHT) for a series of $R(CO)ML_n$ complexes.

At this point, we encounter a problem. Our qualitative model took into account only a limited number of the most important orbitals whereas the EHT method involves all the valence orbitals. Therefore, the question arises: how do we establish correspondence between the results of EHT calculations and those of our qualitative model based largely on the "molecules-in-the-molecules" picture? The solution is to find and compare some qualitative characteristics of the electronic structure in both models. For example, in the framework of the EHT-FMO theory, the charge of the reagent fragment $q(R + CO)$ is a standard characteristic of the electronic structure. On the other hand, in our model, it is obviously connected with the contributions of the two basis configurations Ψ_u and Ψ_r:

$$q(R + CO) = b^2 - 1 = -a^2$$

Indeed, if the mixing vanishes, the reagents remain in their unreactive state ($R^- + CO$), and their total charge is -1, and the total charge of the metal-containing fragment is $+1$. This charge distribution obviously corresponds to the resonance structure Ψ_u. In the resonance structure Ψ_r, the reagents are in their reactive state ($R^{\cdot} + CO$) and their total charge is zero. Clearly, the total charge of the reagents calculated within the FMO-EHT approach does not coincide exactly with that within our model. Electron transfers from and to the reagent (R + CO) orbitals, which were not included explicitly in our treatment, will affect this quantity in the FMO-EHT method. As a result, the total charge of reagents may even be positive. Nevertheless, it is reasonable to think that a smaller negative (and larger positive) charge of the (R + CO) fragment implies a larger contribution of the reactive configuration and therefore the smaller energy barrier for the intraspheric reaction.

The same is correct for the more sophisticated indices: populations of two higher occupied σ-orbitals in the (R + CO) fragment (p_1 and p_2) and their sum Σp. In our model, we included explicitly only two orbitals σ_R and σ_{CO}. To construct the EP for reagents in the framework of our model, we formed bonding and antibonding combinations of two lone pair orbitals (for more details, see [25]). In the unreactive configuration Ψ_u, both combinations are doubly occupied and the indices p_1 and p_2 are both equal to 2, and $\Sigma p = 4$. Abstraction of electrons from these combinations of lone pair orbitals generates the reactive configuration. In the reactive configurations with complete transfer of one electron to the metal-containing fragment, the indices p_1 and/or p_2 are equal to 1. In the framework of the EHT-FMO analysis, the values of the same indices differ. The interpretation, however, remains basically the same. The lone pair orbitals σ_R and σ_{CO} give the main contribution to the two higher occupied σ-MOs of the (R + CO) fragment [8]. Abstraction of electrons from them diminishes the four-electron

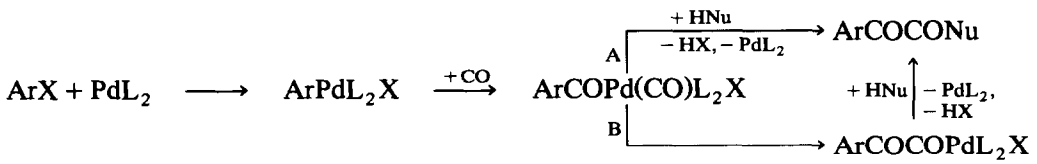

Scheme 5.

TABLE 3. Energies for LUMOs, and mixing indices for a series of metal-containing fragments and activation energies (eV) for CO insertion in their ligand spheres [8]

ML_n^+	E_{LUMO} (eV)	q(R + CO)	p_1	p_2	Σp	ΔE
$Mn(CO)_4^+$	−11.25	+0.17	1.10	1.65	2.75	0.85
$Mn(NO)(CO)_3^{2+}$	−11.34	+0.20	1.09	1.65	2.74	0.71
$Re(CO)_4^+$	−11.17	+0.09	1.16	1.67	2.82	1.42
cis-$Mn(CO)_3PH_3^+$	−11.24	+0.15	1.10	1.66	2.76	0.94
trans-$Mn(CO)_3PH_3^+$	−11.23	+0.16	1.10	1.66	2.76	1.04
$Mn(CO)_2(PH_3)_2^+$	−10.83	+0.16	1.14	1.62	2.76	0.84

destabilizing interaction (exchange repulsion). Electron transfers from and to other orbitals (not considered explicitly in our model) contribute to these indices when calculated within the EHT-FMO approach, but these contributions are not very important because the fraction of the orbitals other than the lone pair orbitals in the two higher occupied MOs of the reagents is minor.

We also found (in the EHT approximation) the energies of the lowest unoccupied MO (LUMO) of ML_n^+ fragments. According to Koopmans' theorem, this energy is equal to minus the EA of the fragment. Since both the reactive species (R^- and CO) and also metal are confined to a single plane throughout the reaction [8,13,15] (reaction plane), and the C_S symmetry is conserved, certain selection rules arise. The LUMO of the metal-containing fragment also must be of the σ-type, as the lone pair orbitals σ_R and σ_{CO} are non-vanishing for the resonance parameter β.

We calculated all the above-mentioned indices for a series of complexes listed in Table 3 and compared them with the calculated activation energy [8] for CH_3 migration in these complexes. For all the complexes, the LUMO of the ML_n fragment was of the σ type. It can be seen from Table 3 that all the indices correlate fairly well with the activation energies calculated in [8] (with the unique exception of the $Mn(CO)_2(PH_3)_2^+$ fragment). Therefore, we conclude that they correctly reproduce the effect of the metal-containing fragment on the CO insertion step.

Then we considered CO insertion in the ligand sphere of $CH_3(CO)M(PH_3)_nCl$ complexes, where M = Ni, Pd, Pt; n = 1, 2 (see Table 4). For all three metals, all the indices suggest that the CO insertion proceeds more easily in the ligand sphere of the four-coordinate $CH_3(CO)M(PH_3)Cl$ complex than in that of the five-coordinate, $CH_3(CO)M(PH_3)_2Cl$. Apparently this result can explain the experimental observation on the carbonylation of RML_2X (Scheme 6). It is known [6,31] that the preferred route involves formation of the intermediate four-coordinated complex RM(CO)LX and then CO insertion in its ligand sphere (path B) rather than transformation of RML_2X to $RCOML_2X$ through the five-coordinated intermediate $RM(CO)L_2X$ (path A).

Another interesting result also can be extracted from the data given in Table 4. Comparing the values of the indices for complexes of different metals, we can see that they do not vary monotonically along the column of the Periodic Table. According to these data,

TABLE 4. Energies for LUMOs, and mixing indices for a series of metal-containing fragments

ML_n^+	E_{LUMO} (eV)	q(R + CO)	p_1	p_2	Σp
$Ni(PH_3)_2Cl^+$	−10.26	−0.36	1.57	1.60	3.17
$Pd(PH_3)_2Cl^+$	−9.67	−0.64	1.62	1.65	3.27
$Pt(PH_3)_2Cl^+$	−10.13	−0.31	1.48	1.61	3.09
$Ni(PH_3)Cl^+$	−10.58	+0.01	1.14	1.76	2.90
$Pd(PH_3)Cl^+$	−10.02	−0.21	1.26	1.79	3.05
$Pt(PH_3)Cl^+$	−10.39	−0.06	1.17	1.74	2.91
$Co(CO)_3^+$	−10.83	−0.04	0.98	1.72	2.70

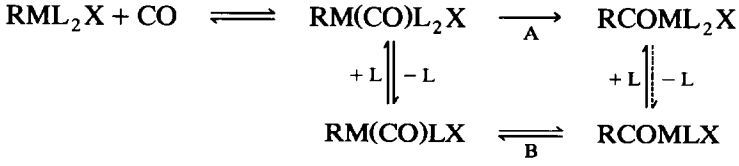

Scheme 6.

the Ni complex is the most reactive, the Pd complex is the least reactive and the Pt complex takes an intermediate position. These conclusions, based upon our approach, are in agreement with experimental results [31].

5. Discussion

The main purpose of our treatment of CO insertion in transition metal complexes was to apply the general approach to reactions of coordinated molecules [21,22] to a process which is extensively studied from different points of view, both experimentally and theoretically. This general approach enabled us to find simple quantities correlating with the reactivity (the reactivity indices) and also to explain the reasons for these correlations.

In the present paper, the approach [21,22] is applied to systems which are largely treated numerically by *ab initio* methods (for recent review see [38]). It has been found that for large scale σ-bonded groups, metals, and ancillary ligands, these simple qualitative considerations work fairly well. In the proposed model, the crucial factors governing the capacity of the transition metal fragment to facilitate the migration of a σ-coordinated ligand to a CO molecule (CO insertion) are the effective IP (measuring the donor capacity or basicity) of the migrating group R^- and the EA (measuring the acceptor capacity or acidity) of the rest of the complex.

The influence of acidity–basicity on CO insertion into the M–Alk and M–Ar bonds has been analysed recently [19] on the basis of extended PRDDO calculations on the CO insertion step. The conclusions [19] concerning the influence of basicity coincide with ours and with those previously presented in the literature [8,14–16]. Basic ligands as a rule (see below however) migrate with ease.

In order to analyse the influence of the acidity of the rest of the metal complex on the insertion reaction, Axe and Marynick [19] have compared the migration in the ligand sphere of manganese and cobalt carbonyls. According to [19], $Co(CO)_4^+$ is a weaker acid than $Mn(CO)_5^+$ and the calculated activation energy is lower for the cobalt complex. It is known from experiment [39] that the migration in the case of the cobalt complex proceeds more easily. Axe and Marynick [19] came to the general conclusion that the migration proceeds more easily in the ligand sphere of weaker acids. The treatment of the acidity effect on the migration rate in the framework of our approach is slightly different from that of [19]. In its scope, the acidity indices (EAs) for other fragments must be compared: not those for $Co(CO)_4^+$ and $Mn(CO)_5^+$, but those for $Co(CO)_3^+$ and $Mn(CO)_4^+$. Unfortunately that comparison also does not favour the Co complex. According to our calculations on $(CH_3)Co(CO)_4$ (see Table 4), the EA suggests that the contribution of the reactive configuration in the case of the Co complex is smaller than that in the case of the Mn complex, thus indicating that the ligand sphere of the $Co(CO)_3^+$ cation proceeds more slowly which contradicts experiment [39] and calculations [19].

On the other hand, it seems to be chemically evident that $Co(CO)_4^+$ is a stronger acid than $Mn(CO)_5^+$. This follows from a comparison of the corresponding hydrides. We can formally consider the carbonylhydrides $HCo(CO)_4$ and $HMn(CO)_5$ as derivatives of the corresponding cations and of the H^- anion. In effect, however, the cobalt derivative evolves the H^+ cations retaining two of the electrons, whereas the manganese derivative evolves atomic hydrogen and retains only one electron. Thus, we conclude that $Co(CO)_4^+$ is a stronger acid. The origin of the above-mentioned discrepancies thus seems to be in certain imperfections of both calculation procedures, which for some reasons are both unable to describe the relative acidity of manganese and cobalt carbonyl complexes.

Attempts to rationalize CO insertion in terms of bond energies are frequent in the literature (see for example [7]). One of the widely used explanations for the inability of some groups to migrate onto coordinated CO is that the energy of the cleaved M–R and M–CO bonds is larger than that of the OC–R and M–COR bonds. That reason is not kinetic in its nature but thermodynamic. It might be valid in some situations; however, a few cases when the acyl nevertheless migrates on the coordinated CO molecule demonstrate its obvious failure. Indeed, the benzoyl ligand migrates in its enolic form in the ligand sphere of the cobalt carbonyl complex, giving the α-enoacyl complex. The α-enoacyl complex then transforms to the α-ketoacyl complex. The energy of the C–C and M–C bonds formed in the case of the benzoyl ($PhCH_2CO$) ligand should not be very different from that of all other aryls which migrate hardly at all. The fact that α-ketoacid nevertheless appears, indicates that the acyl group migration is restricted not thermodynamically but kinetically. In the case where the kinetical restriction is removed by reducing the four-electron repulsion contribution to the energy barrier (for example by the keto-enol transformation), the acyl migration becomes possible.

Usually the restrictions upon the hydride migration are also discussed in terms of bond energies, and for this particular case, that approach has been supported by direct calculations [14]. The C–H bond in the formyl ligand to be formed after insertion is indeed weaker than the M–H bond in the original hydride. If for some accepting group (for example CS), the newly formed

C–H bond is stronger than the original M–H bond, the migration on that terminus is barrierless [14].

Comparing the above facts, we can derive limitations for all the proposed situations, invoking the mixing of $[R^- + CO][ML_n^+]$ and $[R^\cdot + CO][ML_n]$ resonance structures to explain the relative heights of the energy barrier in the intraspheric CO migration. This approach becomes invalid if the basicity of the group R^- expected to migrate or/and acidity of the ML_n^+ fragment are too strong (the IP becomes too small and/or the EA becomes too large). Our approach is based upon a very simple idea that the unreactive configuration $[R^- + CO][ML_n^+]$ is the main contribution to the ground state and therefore the four-electron repulsion controls the energy profile. In that case, certain reductions in the contribution from the unreactive configuration reduce the effect of the four-electron repulsion correspondingly, thus diminishing the energy barrier. If the contribution of this configuration for some reason is small from the beginning (as it can be for example in the case of a hydride complex), the form of the EP is not determined by the four-electron repulsion. Then any variations of that contribution will not affect the EP significantly. In that case, other factors influencing the EP may be important.

One possibility is that the method [21,22] resembles the configuration mixing (CM) approach [23] recently applied to the problem of CO insertion [24]. In the CM approach, the ground state wave function Ψ_G of the reacting system is also presented as a superposition of two electronic configurations,

$$\Psi_G = a\Psi_R + b\Psi_P$$

and the EP for the reaction is also a superposition of the EPs of the two configurations involved. The configurational building blocks Ψ_R and Ψ_P are the electronic configurations of the reagent and the product, respectively. This method of selecting the building blocks is the most general. The method [21,22] uses another procedure for selecting the configurational building blocks Ψ_u and Ψ_r. This procedure (as can be seen from the synopsis) is physically conditioned by the specific origin of the barrier. If the reasons causing the barrier existence are different, the configurations involved in the consideration must also be different. The case of highly basic migrating groups and/or highly acidic ML_n^+ fragments, probably must be treated with some other set of configurations, different from that chosen in the present paper.

The scheme of the treatment (CI) used above to take into account interaction between reactive and unreactive resonance structures is not unique. Specifically, in the case considered, the resonance structures to be mixed differ by the transfer of one electron, and their mixing can be perfectly reproduced in the framework of some MO-LCAO procedures, *e.g.* EHT. This possibility was used when we considered the population indices q, p_i and Σp to characterize the contributions from the reactive and unreactive configurations. For derivation, the configurations were taken as the products of the states of reagents and of the metal-containing fragment. That allowed us to divide the whole problem into tractable parts and to use information on the properties of fragments of the complex, as the method "atoms-in-molecules" does. The indices introduced in the present paper are at least, in principle, more accessible than the EP of the transformation in the whole $R(CO)ML_n$ complex.

Acknowledgements

The authors are grateful to Dr. V.A. Tikhomirov for helpful discussions on the methods of calculation of potential energy surfaces of ionic and radical reactions and to Dr. A.Yu. Cohn for his help during the preparation of the manuscript. A part of this work was performed during a visit of A.L.T. to Cornell University. The hospitality of the Cornell Department of Chemistry is gratefully acknowledged as is the support of the National Science Foundation through the special program for joint US–Russian research (supplement to CHE-8912070). The authors are grateful to Professor R. Hoffmann for encouragement and support.

References

1 M. Röper, in W. Keim (ed.), *Catalysis in C_1 Chemistry*, D. Reidel, Dordrecht, 1983.
2 R. Ugo, in W. Keim (ed.), *Catalysis in C_1 Chemistry*, D. Reidel, Dordrecht, 1983.
3 G. Henrici-Olive and S. Olive, *The Chemistry of Catalyzed Hydrogenation of Carbon Monooxide*, Springer, New York, 1984.
4 Yu.V. Gulevich, N.A. Bumagin and I.P. Beletskaya, *Usp. Khim., 57* (1988) 529 (in Russian).
5 V.F. Calderazzo, *Angew. Chem. Int. Ed. Engl., 16* (1977) 299.
6 G.K. Anderson and R.J. Cross, *Acc. Chem. Res., 17* (1984) 67.
7 J.P. Collman, L.S. Hegedus, J.R. Norton and R.G. Finke *Principles and Applications of Organotransition Metal Chemistry*, University Science Books, Mill Valley, CA, 1987.
8 H. Berke and R. Hoffmann, *J. Am. Chem. Soc., 100* (1978) 7224.
9 D. Saddei, H.-J. Freund and G. Hohlicher, *J. Organomet. Chem., 186* (1980) 63.
10 M.E. Ruiz and A. Flores-Riveros, *J. Catal., 64* (1980) 1.
11 S. Sakai, K. Kitaura, K. Morokuma and K.J. Ohkubo, *J. Am. Chem. Soc., 105* (1983) 2280
12 S. Nakamura and A. Dedieu, *Chem. Phys. Lett., 111* (1984) 243.
13 N. Koga and K. Morokuma, *J. Am. Chem. Soc., 107* (1985) 7230.
14 T. Ziegler, L. Versluis and V. Tschinke *J. Am. Chem. Soc., 108* (1986) 612.
15 N. Koga and K. Morokuma, *J. Am. Chem. Soc., 108* (1986) 6136.
16 F.U. Axe and D.S. Marynick, *Chem. Phys. Lett., 141* (1987) 455.

17 A. Dedieu, S. Sakaki and A. Strich, *Chem. Phys. Lett., 133* (1987) 317.
18 A.K. Rappe, *J. Am. Chem. Soc., 109* (1987) 5605.
19 F.U. Axe and D.S. Marynick, *J. Am. Chem. Soc., 110* (1988) 3728.
20 M.L. McKee, C.H. Dai and S.D. Worley, *J. Phys. Chem., 92* (1988) 1056.
21 A.L. Tchougreeff and I.A. Misurkin, *Dokl. Akad. Nauk SSSR, 291* (1986) 1177.
22 A.L. Tchougreeff and I.A. Misurkin, *Chem. Phys., 133* (1989) 77.
23 A. Pross and S.S. Shaik, *J. Am. Chem. Soc., 104* (1982) 187; S.S. Shaik and A. Pross, *J. Am. Chem. Soc., 104* (1982) 5467; N.D. Epiotis, *Theory of Organic Reactions*, Springer-Verlag, Berlin 1978.
24 A.J. Shusterman, I. Tamir and A. Pross, *J. Organomet. Chem., 340* (1988) 203.
25 A.L. Tchougreeff, Yu.V. Gulevich, I.A. Misurkin and I.P. Beletskaya, *Metallorg. Khim., 1* (1988) 1159 (in Russian).
26 R. Hoffmann, *Solids and Surfaces: A Chemist's View of Bonding in Extended Structures*, VCH, New York, 1988.
27 R. Hoffmann, M. Kersting and Z. Nomicou, *J. Chem. Phys., 95* (1991) 4033.
28 K. Fukui, N. Koga and H. Fujimoto, *J. Am. Chem. Soc., 103* (1981) 196; H. Fujimoto, N. Koga and I. Hatane, *J. Phys. Chem. 88* (1984) 3539; H. Fujimoto, T. Yamasaki, I. Hatane and N. Koga, *J. Am. Chem. Soc., 89* (1985) 779.
29 I.P. Goldshtein, I.A. Misurkin, N.V. Varentsova, I.E. Paleeva, E.S. Shcherbakova and E.N. Gur'yanova, *Zh. Obshch. Khim. SSSR, 51* (1981) 2087; Ju.A. Panteleev and A.A. Krasheninnikov, Teor. Eksp. Khim., 13 (1977) 100 (both in Russian).
30 V.N. Kondratiev (ed.), *Bond Energies, Ionization Potentials, and Electron Affinities*, Nauka, Moscow, 1974 (in Russian).
31 P.E. Garrou and R.F. Heck, *J. Am. Chem. Soc., 98* (1976) 4115.
32 R.J. Angelici, *Acc. Chem. Res., 5* (1972) 335.
33 F. Ozawa, H. Soyama, H. Yanashihara, I. Aoyama, H. Takino, K. Izawa, T. Yamamoto and A. Yamamoto, *J. Am. Chem. Soc., 107* (1985) 3235; F. Ozawa, L. Huang and A. Yamamoto, *J. Organomet. Chem., 334* (1987) C9.
34 J.T. Chen and A. Sen *J. Am. Chem. Soc., 106* (1984) 1506; A.J. Sen, J.T. Chen, W.M. Vetter and R.J. Whittle *J. Am. Chem. Soc., 109* (1987) 148.
35 F. Francalanci, A. Gardano, L. Abis, T. Fiorani and M. Foa, *J. Organomet. Chem., 243* (1983) 87.
36 R. Hoffmann, H. Fujimoto, J.R. Swenson and C.-C. Wan, *J. Am. Chem. Soc., 95* (1973) 7644.
37 R. Hoffmann and W.N. Lipscomb *J. Chem. Phys., 36* (1962) 2179; R. Hoffmann and W.N. Lipscomb, *J. Chem. Phys., 36* (1962) 3489; R. Hoffmann, *J. Chem. Phys., 39* (1963) 1397.
38 N. Koga and K. Morokuma, *Chem. Rev., 91* (1991) 823.
39 Z. Nagy-Maros, G. Bor and L. Marko, *J. Organomet. Chem., 14* (1968) 205.